HHS Public Access

Author manuscript

Mol Psychiatry. Author manuscript; available in PMC 2016 November 01.

Published in final edited form as:

Mol Psychiatry. 2016 May ; 21(5): 615–623. doi:10.1038/mp.2015.103.

Nonmuscle myosin IIB as a therapeutic target for the prevention of relapse to methamphetamine use

Erica J. Young, PhD[1,2,*], **Ashley M. Blouin, PhD**[1,2,*], **Sherri B. Briggs, PhD**[1,2,*], **Stephanie E. Daws, PhD**[1,2], **Li Lin, PhD**[3,4], **Michael D. Cameron, PhD**[3,4], **Gavin Rumbaugh, PhD**[2], **Courtney A. Miller, PhD**[1,2,#]

[1]Department of Metabolism & Aging

[2]Department of Neuroscience

[3]Drug Metabolism and Pharmacokinetics, Translational Research Institute

[4]Department of Molecular Therapeutics, The Scripps Research Institute, Jupiter, FL USA

Abstract

Memories associated with drug use increase vulnerability to relapse in substance use disorder (SUD) and there are no pharmacotherapies for the prevention of relapse. Previously, we reported a promising finding that storage of memories associated with methamphetamine (METH), but not memories for fear or food reward, is vulnerable to disruption by actin depolymerization in the basolateral amygdala complex (BLC). However, actin is not a viable therapeutic target because of its numerous functions throughout the body. Here we report the discovery of a viable therapeutic target, nonmuscle myosin II (NMIIB), a molecular motor that supports memory by directly driving synaptic actin polymerization. A single intra-BLC treatment with Blebbistatin, a small molecule inhibitor of class II myosin isoforms, including NMIIB, produced a long-lasting disruption of context-induced drug seeking (at least 30 days). Further, post-consolidation genetic knockdown of *Myh10*, the heavy chain of the most highly expressed NMII in the BLC, was sufficient to produce METH-associated memory loss. Blebbistatin was found to be highly brain penetrant. A single systemic injection of the compound selectively disrupted the storage of METH-associated memory and reversed the accompanying increase in BLC spine density. This effect was specific to METH-associated memory, as it had no effect on an auditory fear memory. The effect was also independent of retrieval, as METH-associated memory was disrupted twenty-four hours after a single systemic injection of Blebbistatin delivered in the home cage. Together, these results argue for the further development of small molecule inhibitors of nonmuscle myosin II as potential therapeutics for the prevention of SUD relapse triggered by drug associations.

[#]**Correspondence:** Courtney A. Miller, cmiller@scripps.edu, 130 Scripps Way, Jupiter, FL 33477, 561-228-2958 (phone and fax).
[*]Equal contribution

CONFLICT OF INTEREST

The authors have no conflicts of interest to report.

Supplementary information is available at *Molecular Psychiatry's* website.

Keywords

Actin; memory; synapse; retrieval; addiction; drug seeking

INTRODUCTION

Substance use disorder (SUD) is a chronic, relapsing disorder. Thus, a major challenge facing the treatment of SUD is preventing relapse after patterns of drug seeking behavior have become deeply engrained. During drug use, a multitude of associations form between the drug and stimuli present at the time, which can range from drug paraphernalia to components of the environment in which the drug is used (1). The associations become highly motivating on their own, such that they can serve as rapid, conscious or unconscious triggers to seek out the drug. Perhaps most troubling, these drug-associated stimuli can retain their ability to motivate drug seeking behavior, even after seemingly successful rehabilitation and prolonged drug-free periods.

Pharmacotherapeutic options for SUD are extremely limited. A few, moderately effective replacement therapies exist for opiate, nicotine and alcohol dependence. However, no such options exist for psychostimulant dependence and, further, there are no pharmacotherapies for the prevention of relapse associated with any drug of abuse. Current behavioral modification strategies commonly employ exposure therapy, a form of memory extinction that targets each trigger by accelerating learning of a new, non-reward contingency for each associated stimulus (2). Research efforts are directed at identifying molecular accelerators of extinction to increase the speed and efficacy of exposure therapy (3–8). However, because exposure therapy leaves the original drug-associated memory intact, the therapeutic efficacy of this approach is limited by the constant potential for spontaneous renewal of the conditioned drug seeking response. A strategy being developed to more permanently alter drug-associated memories takes advantage of reconsolidation, a short period of time following retrieval when a memory is susceptible to disruption (9–14). However, the triggers for drug-associated memories can be numerous for an individual and often unconscious or abstract (15), suggesting that the retrieval-based strategies of extinction and reconsolidation may have limited efficacy. An alternative approach might be one that does not rely on retrieval, instead targeting drug-associated memories while in storage. However, in the absence of retrieval, this poses a new challenge of how to selectively target SUD associations without disrupting the countless other memories that have accumulated throughout life. Recently, we identified an actin-based mechanism employed by the brain to store memories associated with the psychostimulant methamphetamine (METH) (16).

Dendritic spines, the small, but highly dynamic postsynaptic structures found at the majority of forebrain excitatory synapses, are thought to be the structural site of memory storage (17). At the time of memory formation, dendritic spines facilitate signal integration and information storage by enabling input-specific biochemical and electrical isolation of synapses. Furthermore, volumetric and functional changes of dendritic spines are critical for the successful formation of long-term memories (18, 19). The workhorse of this structural and functional plasticity is actin polymerization, the process of linking actin monomers (G-

actin) into complex, branched filaments (F-actin) (20, 21). These actin filaments comprise the cytoskeleton in dendritic spines and are surprisingly dynamic, capable of making rapid structural changes on the order of seconds (22–26). Indeed, disrupting learning-induced F-actin dynamics at the time of training prevents the formation of long-term fear memories (25, 27–30). Findings from synaptic plasticity and fear memory studies indicate that F-actin dynamics are under tight temporal control, such that actin rapidly stabilizes after synaptic stimulation. This renders the cytoskeleton and associated synaptic potentiation and memory invulnerable to disruption by actin depolymerizing agents, such as Latrunculin A, within minutes of stimulation (22, 29, 30). However, recent evidence from our lab suggests that the F-actin supporting METH-associated memories remains dynamic long after learning, presenting an unanticipated weakness of these pathogenic associations (16). Indeed, METH-associated memories can be selectively disrupted through actin depolymerization in a subregion of the amygdala, the brain's emotional memory center, long after learning has occurred and in the absence of retrieval. Importantly, the same manipulation has no effect on associative memories for fear or food reward. Further, METH-associated memory is accompanied by an increase in spine density in the basolateral amygdala complex (BLC) that is reversed by actin depolymerization, corresponding to loss of the memory.

Given these results, actin depolymerization would seem to be a promising therapeutic target, particularly given that a single treatment with Latrunculin A is sufficient to immediately disrupt METH-associated memories. However, β-actin, the isoform implicated in adult neuronal structural plasticity, is ubiquitously expressed throughout the body and is critical for a multitude of processes, such as cell polarity, adhesion and migration. Because of the limitations associated with actin depolymerization as a therapeutic, we have turned our efforts toward identification of upstream regulators of the synaptic actin cytoskeleton in hopes of identifying a viable therapeutic target for the selective disruption of METH-associated memory. These efforts have led to the myosin family, which is comprised of 143 molecular motors spread over seventeen different classes, each with tissue-specific properties (31). We focused our investigation on nonmuscle myosin II (NMII), a myosin subclass and ATP-dependent molecular motor we have previously demonstrated to play a crucial, temporally restricted role in synaptic actin polymerization and fear memory (25, 30).

MATERIALS AND METHODS

All procedures were performed in accordance with the Scripps Research Institute Animal Care and Use Committee and national regulations and policies.

Drugs

Methamphetamine hydrochloride (Sigma-Aldrich) was delivered IV at 0.02 mg in a 0.05 ml infusion to rats for self-administration and IP at 1.0 mg/kg to rats or 2.0 mg/kg to mice for CPP. Both enantiomers of Blebbistatin (Blebb; − = active Blebb, + = inactive Blebb [Vehicle control]; Calbiochem) were infused into the BLC at a concentration of 90ng/μl in 10% DMSO and 0.9% saline. To address poor solubility of active (−) Blebb, racemic (+/−) Blebb (Tocris) was used for IP injections. It was diluted to 1 mg/ml in a vehicle of 0.9% saline

and 6.7% DMSO/25% Hydroxypropyl β-Cyclodextrin (HPβCD) and delivered to mice at 10 mg/kg.

Intra-BLC infusions were delivered at a rate of 0.25 μl/min over 2 min for rats and 0.15 μl/min over 2 min for mice. Infusers were left in place for 1 min to allow for diffusion of the drug away from the needle tip. At the completion of behavioral procedures, 40 μm sections were stained with cresyl violet to verify placement of the infusion needle tips within the BLC (Supplemental Figure S1).

Pharmacokinetics

See Supplementary Information

Behavioral Procedures

Self-Administration—There were four different phases of self-administration: food training, METH training, extinction and reinstatement. Prior to catheter/guide cannula implantation and the start of self-administration training, all rats underwent food training. METH self-administration training was conducted during 2 hour sessions for 14 consecutive days in Context A. Animals were trained to press the active lever on a Fixed Ratio schedule of 1 (FR1) for METH reinforcement, followed by a 20 sec time-out period. Lever presses on the inactive lever were not reinforced. Animals moved on to the extinction phase after achieving a minimum average of 10 METH infusions per day over 14 consecutive days. Extinction training consisted of 2 hour sessions free of reinforcement conducted in Context B. Animals were assigned to a different operant chamber during extinction. Reinstatement testing took place in Context A for 1 hour, starting 24 hours after the last day of extinction. Animals underwent 3 reinstatement tests: 1 day (R1), 2 days (R2) and 30 days (R30) following extinction. 30 min prior to reinstatement day 1 (R1), animals received one intra-BLC infusion of (−) Blebb or (+) Blebb (vehicle control).

Conditioned Place Preference—CPP was performed as previously described (16, 32, 33). For mice, the protocol consisted of three phases: pretesting, training and testing. Pretesting took place over 2 days, during which mice were allowed to freely explore the CPP apparatus for 30 min each day. The first 30 min session and the first 15 min of the second session served as a habituation period to allow the mice to acclimate to the novel context without inducing latent inhibition, while the final 15 min period was used to assess pre-drug compartment preference. Mice were trained over four consecutive days with twice daily training sessions, such that mice received both METH (2mg/kg) and saline each day. Randomization was performed such that starting chamber, initial preference and time of day for METH treatment were counterbalanced within groups. Further, each mouse cage was counterbalanced between control and treatment groups. Testing consisted of 15 min free access to the CPP apparatus and was conducted at least two days after the final day of training. See Supplementary Information for additional details regarding rat CPP.

Fear Conditioning—Modified mouse Noldus Phenotypers were used for auditory fear conditioning. Mice were first habituated to the training context for a total of 12 minutes over three exposures in one day. For training, mice explored the chamber for 3 minutes before

receiving 3 pairings of a 30 sec auditory tone (6kHz, 85dB) that coterminated with a foot shock (1 sec, 0.5mA). For testing, mice explored the novel test context for 3 min, 48 hours after training, followed by three 30 sec presentations of the tone with a 30 sec inter-trial interval. Freezing behavior was assessed during each 30 sec tone presentation and averaged across the three tones.

See Supplementary Information for additional Behavioral Procedure details.

RNA Sequencing

RNA-Seq was performed on tissue isolated from 8–12 week old naïve male mice. RNA was extracted from the BLC with the miRVANA PARIS RNA kit (Life Technologies, Carlsbad, CA) and 100 ng from each sample (N=4) was used for library preparation with the TruSeq RNA Sample Prep Kit (Illumina, San Diego, CA). Library preparation and 150 bp paired-end sequencing on the Illumina NextSeq 500 were performed by the Scripps Florida Genomics Core. Reads were mapped to the genome using TopHat/Bowtie software(34, 35) and normalized means were obtained using the DeSeq package (36) in Bioconductor. RPKM values were used to determine basal levels of myosin II heavy chains.

shRNA and siRNA-mediated focal knockdown of *Myh10* (NMIIB)

One month before the start of training, rats were injected with 1.0 μl of recombinant adeno-associated virus (rAAV2/5) expressing either eGFP alone or a short hairpin RNA (shRNA) against *Myh10* (nonmuscle myosin IIB heavy chain) that also expressed wtGFP. Bilateral injections were delivered to the BLC (AP: −2.9mm, ML ± 5mm from bregma; DV −8.7mm from skull) at a rate of 0.13 μl/min using an automated injection pump through a 10μL syringe and 33-gauge stainless steel needle (Hamilton Company Reno, Nevada). Tissue was collected 72 hours after testing to confirm MYH10 knockdown. See prior publications for additional details on viruses and images of injection site (9, 18, 23).

Knockdown of *Myh10* with small interfering RNA (siRNA) was first assayed in naïve mice 24 hrs after intra-BLC injection of the appropriate siRNA pool (ON-TARGETplus SMARTpool, mouse *Myh10* or nontargeting pool; Dharmacon, Waltham, Maryland; see Supplementary Table 1 for target sequences) using JetSI transfection reagent (Polyplus Transfection, Illkrich, France) (33, 37–39). The appropriate siRNA-JetSI complexes were injected bilaterally into the BLC (AP: 1.5 mm, ML: ±3.2 mm from bregma and DV: − 4.7 mm from skull) at 1 μL at 200 nL/min in the same way that shRNA-AAVs were injected. In a separate group of mice used for behavioral testing, *Myh10* or control siRNAs were infused into the BLC through bilateral guide cannulae after training, as described above. For additional details regarding confirmation of knockdown, see Supplementary Information.

Quantitative Reverse-Transcriptase Polymerase Chain Reaction and Immunoblotting

See Supplementary Information.

Spine Density Analysis

See Supplementary Information.

Statistical Analysis

Wilcoxon signed rank tests were used to assess CPP compartment preferences (32, 40–44). One-way analysis of variance and repeated measures ANOVAs were used for all other experiments, with Tukey's post hoc tests when appropriate. The Shapiro-Wilks normality test and Levene test were used to verify that all datasets met the criteria for normal distribution and equal variance, respectively. Statistical significance was set at $P \leq 0.05$ and variation is presented as standard error of the mean.

RESULTS

Inhibition of amygdalar myosin II produces a long-lasting disruption of context-induced drug seeking

We recently demonstrated that intra-BLC Blebb, a small molecule inhibitor of class II myosin isoforms, including NMIIs (45), disrupted METH conditioned place preference (CPP) (16). Therefore, we first sought to address the potential for Blebb to produce a long-lasting disruption of drug seeking by using a gold standard model of memory-induced drug seeking, context-induced reinstatement of instrumental lever pressing for METH (46–49). After training in Context A and extinction in Context B (Figure 1a and b), rats were returned to Context A for reinstatement (Figure 1c; Overall Active Lever: $F_{(1,12)}=22.22$, $P<0.0005$; Overall Inactive Lever: $F_{(1,12)}=0.18$, $P>0.05$). Reexposure to the METH-paired context reinstated drug seeking in controls, but not those that received Blebb infusions targeted at the BLC prior to testing (R1 Active Lever: $F_{(1,12)}=8.49$, $P<0.05$). As with Latrunculin A (16), inhibiting myosin II also prevented METH seeking in a subsequent Blebb-free test session twenty-four hours later (Figure 1c; R2 Active Lever: $F_{(1,12)}=4.83$, $P<0.05$). Furthermore, the single Blebb infusion prior to Reinstatement Test 1, produced a long-lasting disruption of drug seeking, such that lever pressing was still attenuated at a third reinstatement test 30 days later (Figure 1c; R30 Active Lever: $F_{(1,12)}=23.49$, $P<0.0005$). This long-lasting effect indicates that spontaneous recovery of the memory did not occur.

The nonmuscle myosin IIB isoform is required to maintain a METH-associated memory

Several different myosins are expressed in the brain, including members of the myosin II class. In addition to NMIIs, Blebb inhibits skeletal, cardiac and some smooth muscle myosin IIs (45, 50–52). Baseline gene expression analysis by RNA sequencing indicates that no skeletal muscle isoforms of myosin II are present in the BLC of adult mice. However, the genes encoding the heavy chains of two of the cardiac muscle myosin II's, *Myh7* and *Myh7b*, are expressed, along with the smooth muscle myosin heavy chain (*Myh11*) and all three NMII isoforms, *Myh9* (NMIIA), *Myh10* (NMIIB) and *Myh14* (NMIIC), with *Myh10* being the most highly expressed ($F_{(5,18)}=47.44$, $P<0.0001$; Figure 2a). Proteomic analyses have indicated that all five of these myosin II heavy chains are expressed at the synapse and we have previously reported that cardiac *Myh7b*, while expressed at very low levels in the brain, is capable of regulating hippocampal dendritic spine synapse structure and function (53–55). Therefore, while our previous findings related to fear memory formation suggest the current effects of Blebb on METH-associated memory are likely mediated through the most abundant myosin II, NMIIB (*Myh10*; (25, 30)), we cannot be certain if a specific myosin II isoform is responsible.

To address this, we first used an rAAV vector expressing an shRNA targeting *Myh10* to determine whether the specific NMII isoform, NMIIB, supports a METH-associated memory in the BLC (Figure 2b; (25)). Importantly, there were no differences between control and *Myh10* shRNA animals in pre-training preference for either CPP compartment in terms of time spent in the black versus white side (Figure 2c; RM-ANOVA, $F_{(1,18)}$=0.16, P>0.05), consistent with an "unbiased" protocol, nor was there a difference once the animals had been randomly assigned so that an equal number had the CS+ paired with the black side, as with the white. Thus, all animals received METH in their least pre-training preferred compartment to avoid introducing any potential bias to post-training preference (CS+ Control shRNA: 330.3 sec ± 10.6, *Myh10* shRNA: 333.7 sec ± 11.8; CS- Control shRNA: 380.9 sec ± 10.5, *Myh10* shRNA: 385.5 sec ± 20.0; RM-ANOVA, $F_{(1,18)}$=0.16, P>0.05). Further, locomotion was equivalent between groups during the Pretest when initial preference was established and during the post-training test (see Supplementary Table 2). Animals treated with the control shRNA displayed a robust METH-associated memory at testing, preferring the drug-paired context (Conditioned Stimulus, CS+) over the saline-paired context (CS−), whereas animals treated with the *Myh10* shRNA showed no evidence of a preference (Figure 2d; Control shRNA: z=−2.67, P<0.05; MyH10 shRNA z=−0.051, P>0.05). In subsequent tissue analysis, we confirmed that MYH10 protein levels were significantly reduced in the BLC of rats injected with the *Myh10* shRNA (Figure 2e: $F_{(1,18)}$=5.0, P<0.05), without affecting mRNA levels of the closely associated NMIIA and NMIIC heavy chains, *Myh9* ($F_{(1,8)}$=0.107, P>0.05) and *Myh14* ($F_{(1,8)}$=0.991, P>0.05; Figure 2f;). These results indicate that NMIIB is required for METH-associated memory. However, this does not address NMIIB's contribution to the specific phase of memory storage.

To more precisely examine the contribution of NMIIB to the maintenance of a METH-associated memory, we used siRNA-mediated acute focal knockdown of *Myh10* in the BLC. Using naïve adult mice, we first confirmed effective knockdown of MYH10 protein *in vivo* 24 hours after intra-BLC siRNA injection, as compared to a nontargeting control siRNA (Figure 3a, P<0.005). Interestingly, MYH10 levels had already begun to recover to baseline levels by 48 hours post-siRNA injection, indicating a rapid turnover rate for *Myh10* (Figure 3a). To achieve the necessary temporal control over MYH10, the appropriate siRNA pool was infused into the BLC one day after the final training session and METH-associated memory was assessed twenty-four hours later (Figure 3b–c), a time point at which the NMII heavy chain was significantly knocked down (Figure 3a). Mice that received intra-BLC infusions of the nontargeting control siRNA showed a robust preference for the drug-paired compartment. However, mice that received the *MyH10* siRNA demonstrated no such preference (Figure 3c; Overall: $F_{(1,24)}$=9.36, P<0.005; Control vs *Myh10* T1: $F_{(1,24)}$=11.82, P < 0.005). This effect persisted into a subsequent test twenty-four hours later, despite the rapid recovery rate of MYH10 from siRNA-mediated knockdown ($F_{(1,24)}$=3.95, $P \leq 0.05$; Figure 3a). This latter finding is consistent with results obtained with Blebb, pointing to the acute nature of NMIIB inhibition's ability to produce a persistent METH-associated memory disruption. And again, as with the *Myh10*-AAV, no differences in locomotion were present between the experimental and control groups (Supplementary Table 2). Further, there was

no effect of the *Myh10* siRNA on *Myh9* ($F_{(1,3)}$=0.98, *P*>0.05) or *Myh14* mRNA levels ($F_{(1,3)}$=0.236, *P*>0.05; Figure 3d).

METH-associated memory storage can be selectively targeted from the periphery with a myosin II inhibitor

The Topological Polar Surface Area (TPSA), an *in silico* calculation of the molecular surface area of all polar atoms (56), of Blebb is reported in PubChem to be 52.9 A^2. Generally, compounds with a TPSA lower than 90 A^2 are expected to have high brain penetrance (57). Therefore, given the therapeutic potential of a systemic drug delivery option for SUD relapse, we investigated the ability of systemically administered Blebb to cross the blood brain barrier and disrupt METH-associated memory.

As an initial *in vivo* screen, we assessed the effect of a single intraperitoneal (IP) injection of Blebb on tissue distribution and several measures of health in mice. Unfortunately, solubility issues precluded the use of the pure active enantiomer of Blebb. Indeed, a thermodynamic solubility test confirmed this issue, with a noticeable precipitate observed with the pure enantiomer, but not racemate, immediately upon addition of DMSO stock. The final concentration after twenty-four hours was 315 μM for the pure enantiomer and 924 μM for the racemate. Thus, racemic Blebb was used at 10 mg/kg, delivering 5 mg/kg of the active enantiomer. Tissue was collected fifteen and forty-five minutes after IP injection. As anticipated, there was excellent brain penetrance, as determined by the brain to plasma ratio (Supplementary Table 3). Acute effects of the compound were monitored in a separate group of mice for two hours post-IP injection. Blebb had no apparent effects on any of the health measures (Supplementary Table 4), which were selected and ratings developed based on previously published methods for phenotyping mice after pharmacologic and genetic manipulations (58).

In a parallel set of experiments, microsomal stability and *in vivo* pharmacokinetic properties of Blebb were determined by IV injection of the pure active enantiomer (1mg/kg) and plasma collection at several time points over eight hours post-injection. Blebb displayed poor microsomal stability, particularly in rat and mouse (Supplementary Table 5). Further, Blebb was rapidly cleared from plasma, with undetectable levels by 60 minutes post-injection (Supplementary Table 5). Shortly after IV injection, a sharp decline in motor function was noticed and maintained for the first 30 minutes. Full recovery was seen by 60 minutes post-injection, presumably when the drug had cleared. This was unexpected, as mice given 10 mg/kg of racemic Blebb showed normal behaviors during the same post-injection time frame (Supplementary Table 4), including normal locomotion during the first 30 minutes (Distance – Veh: 12973.98cm ± 877.1, Blebb: 11936.55 ± 1930.5, *P*=0.64; Velocity – Veh: 7.39 cm/s ± 0.50, Blebb: 6.76 cm/s ± 1.05, *P*=0.61). These results indicate a narrow therapeutic index for Blebb, perhaps due to its actions on cardiac myosin IIs. Further, it suggests that only a strikingly brief window of myosin II inhibition may be necessary to produce a lasting disruption of METH-associated memory. Additional experiments will be needed to determine the rate of clearance from the brain.

Using the same dose and route of administration as was used to assess the health effects and brain penetrance of Blebb, we determined the impact of systemically administered Blebb

on a consolidated METH-associated memory. Two days after the final METH CPP training session, a single IP injection of Blebb was administered 30 minutes prior to assessment of METH-associated memory in the absence of METH reinforcement (Figure 4a). Vehicle-treated controls displayed a strong METH-associated memory, preferring the previously drug-paired context (CS+) over the saline-paired context (CS−) (Figure 4b; $z=-2.16$, $P<0.05$). However, similar to intra-BLC LatA and Blebb in rats (16), systemic Blebb-treated mice displayed an immediate memory disruption (Figure 4b; $z=-0.79$, $P>0.05$), with no effect on locomotion (Supplementary Table 2).

METH-associated memory is accompanied by an increase in BLC spine density that is reversed by an intra-BLC infusion of Latrunculin A (16). Importantly, Latrunculin A has no effect on spine density in control, saline-treated mice (16). Therefore, we next sought to determine if the memory disrupting effects of systemic Blebb were accompanied by a similar decrease in BLC spine density. Following the behavioral testing depicted in Figure 4b, the BLC of these vehicle or Blebb-treated Thy1-GFP(m) mice was imaged and spine density determined (Figure 4c). Thy1-GFP(m) mice express eGFP in forebrain pyramidal neurons with clear labeling in the BLC (16, 59). All dendrites chosen for spine density analysis were comparable in width across groups ($F_{(1,10)}=1.22$, $P>0.05$). METH-associated memory loss induced by systemic myosin II inhibition was accompanied by a significant reduction in BLC spine density compared to control METH CPP animals that received vehicle infusions prior to testing (Figures 4c; $F_{(1,10)}=4.8$, $P<0.05$). The effect size was strikingly similar to that of Latrunculin A (16).

Pre-training intra-BLC Blebb disrupts the formation of an auditory fear memory. However, when given prior to testing, this same drug treatment has no effect on auditory or contextual fear memories (25, 29, 30). Therefore, we next addressed the selectivity of systemic Blebb for a drug-associated memory by assessing the effects on fear memory. Systemic Blebb had no effect on the expression of a previously consolidated, BLC-dependent auditory fear memory (Figure 4d and e; $F_{(1,24)}=1.61$, $P>0.05$) or spine density (Figure 4f; $F_{(1,8)}=0.17$, $P>0.05$), which is increased in the BLC with fear memory (60, 61). All dendrites chosen for spine density analysis were comparable in width across groups ($F_{(1,8)}=1.99$, $P>0.05$). Taken together, these results indicate that Blebb is able to cross the blood brain barrier at a high enough concentration to inhibit myosin II and alter METH-associated memory (Figure 4b) and spine density (Figure 4c), while leaving fear memory and fear memory-associated spines intact (Figure 4e and f).

A therapeutic advantage of targeting the actin cytoskeleton is that its effect on METH-associated memory does not depend upon retrieval. To determine if myosin II inhibition is capable of disrupting the storage of a METH-associated memory in the absence of retrieval, mice received a single systemic injection of Blebb in the home cage two days after the completion of training (Figure 5a). Twenty-four hours later, Blebb-treated mice displayed no METH-associated memory (Figure 5b; Vehicle: $z=-2.20$, $P<0.05$; IP Blebb: $z=0.0$, $P>0.05$). Two weeks later, the same animals were trained for auditory fear conditioning and tested the following day in the absence of any drug treatment (Figure 5a). Animals that previously underwent an IP Blebb-induced disruption of METH-associated memory expressed an auditory fear memory equal in strength to previously vehicle-treated controls (Figure 5c;

$F_{(1,13)}$=0.28, P>0.05), indicating that prior Blebb treatment did not disrupt the brain's ability to form future memories.

DISCUSSION

In a prior study, we discovered that the storage of METH-associated memories appears to be governed by a unique state of continuously cycling actin (16), unlike other types of amygdala-dependent memories that are supported by an actin cytoskeleton that stabilizes within minutes of learning (25, 30). Unfortunately, the therapeutic potential of this finding was limited because direct targeting of actin polymerization via peripheral drug administration would have lethal side effects. Indeed, many toxins found in nature potently target actin-based cytoskeletal dynamics. Here we report a critical advance by identifying a viable target for achieving actin depolymerization, nonmuscle myosin IIB, to serve as the foundation for future neurotherapeutic development. Indeed, systemic delivery of the myosin II inhibitor, Blebbistatin, reliably and selectively disrupted the storage of METH-associated memory and associated structural plasticity. Myosin II's canonical function is to drive retrograde actin flow in growth cones of developing neurons by imparting a shearing force on them (62). If myosin II function is lost, the flow of actin stops, and the growth cone collapses. Additionally, we have previously demonstrated that the nonmuscle myosin IIB isoform participates in structural reorganization of the spine actin cytoskeleton in response to synaptic stimulation by applying a similar mechanical force to drive F-actin polymerization (25). This reorganization is rapid, complete within minutes of stimulation, and supports the stable expression of LTP, as well as hippocampus and amygdala-dependent fear memories (25, 30). Contrary to its role in these more traditional forms of plasticity and memory, our current study suggests that NMIIB remains constitutively active in support of METH associations, continuing to drive actin polymerization, such that memories associated with METH can be selectively targeted without the need for retrieval days to weeks after learning.

Immediately following withdrawal, most substance users enter a "honeymoon" phase where they report feeling physically and emotionally well, with few cravings (63). However, approximately one to three months into recovery, many abstinent individuals report hitting a "wall". This phase of recovery is marked by anhedonia and strong cravings that often result in relapse (63). A comparable pattern of behavior, termed the incubation of craving, has been observed in animal self-administration models where motivation to drug seek can increase over the course of thirty days of forced abstinence (64–66). Time-dependent adaptations of nucleus accumbens glutamatergic synapses are known to partially mediate this effect and recent evidence indicates that this is modulated by silent synapses on glutamatergic projections from the amygdala and prefrontal cortex (67–69). Indeed, despite the extinction effects of repeated reinstatement testing in the current study, the animals treated with the inactive enantiomer of Blebb (Vehicle; Figure 1) showed no sign of reduced drug seeking from the first (R1) to the final reinstatement (R30) sessions, suggesting a powerful drive to seek METH more than a month after drug cessation. Animals given a single treatment with the active enantiomer of Blebb (Blebb; Figure 1), on the other hand, showed no sign of spontaneous recovery of the drug seeking response over the "incubation

of craving" period, demonstrating a strong and long-lasting disruption of METH-associated memories by myosin II inhibition.

Blebb is the only small molecular inhibitor of nonmuscle class II myosins and was found through a small scale screen (70). The paucity of myosin II small molecule inhibitors is surprising because these heavily studied molecular motors are integral to a number of cell biological processes. In addition to its efficacy in our SUD animal models, several aspects of Blebb suggest that it is an excellent starting point for medicinal chemistry efforts. Blebb is brain penetrant (Supplementary Table 3), has a low molecular weight (292.3 g/mol), and a single dose is sufficient to disrupt a METH-associated memory. Further, phototoxicity reported with Blebb upon exposure to blue light was recently overcome with a C15 nitro derivative of the compound (71). However, several aspects of Blebb are still in need of improvement from a neurotherapeutic perspective, particularly its selectivity and solubility. In addition to being an inhibitor of all three nonmuscle myosin II isoforms (A, B and C), Blebb targets skeletal, smooth and cardiac muscle myosin IIs, which are expressed in the adult human amygdala (72) and throughout the body. Therefore, future medicinal chemistry efforts directed at improved isoform selectivity would provide biologists with much needed nonmuscle myosin II probes and benefit SUD neurotherapeutic discovery.

Supplementary Material

Refer to Web version on PubMed Central for supplementary material.

Acknowledgments

The authors thank the Scripps Florida Genomics Core for their assistance with RNA sequencing, the Scripps Florida Behavior Core for providing behavioral equipment, Dr. Christine Gall for her helpful comments and Colton Hoffer for technical assistance. This work was supported by grants from the National Institute on Drug Abuse (R01DA034116, R01DA034116S1 and R21DA036376 to CAM), National Institute for Neurological Disorders and Stroke (R01NS064079 to GR) and National Institute for Mental Health (R01MH096847 to GR) and the Brain and Behavior Research Foundation (NARSAD Young Investigator Awards to AMB and SED).

References

1. Childress AR, Mozley PD, McElgin W, Fitzgerald J, Reivich M, O'Brien CP. Limbic activation during cue-induced cocaine craving. The American journal of psychiatry. 1999; 156 (1) 11–8. [PubMed: 9892292]
2. Phillips KA, Epstein DH, Preston KL. Psychostimulant addiction treatment. Neuropharmacology. 2014; 87C: 150–60.
3. Price KL, Baker NL, McRae-Clark AL, Saladin ME, Desantis SM, Santa Ana EJ, et al. A randomized, placebo-controlled laboratory study of the effects of D-cycloserine on craving in cocaine-dependent individuals. Psychopharmacology (Berl). 2013; 226 (4) 739–46. [PubMed: 22234379]
4. Botreau F, Paolone G, Stewart J. d-Cycloserine facilitates extinction of a cocaine-induced conditioned place preference. Behav Brain Res. 2006; 172 (1) 173–8. [PubMed: 16769132]
5. Malvaez M, McQuown SC, Rogge GA, Astarabadi M, Jacques V, Carreiro S, et al. HDAC3-selective inhibitor enhances extinction of cocaine-seeking behavior in a persistent manner. Proc Natl Acad Sci U S A. 2013; 110 (7) 2647–52. [PubMed: 23297220]
6. Myers KM, Carlezon WA Jr, Davis M. Glutamate receptors in extinction and extinction-based therapies for psychiatric illness. Neuropsychopharmacology. 2011; 36 (1) 274–93. [PubMed: 20631689]

7. Peters J, Kalivas PW, Quirk GJ. Extinction circuits for fear and addiction overlap in prefrontal cortex. Learn Mem. 2009; 16 (5) 279–88. [PubMed: 19380710]
8. Bird MK, Lohmann P, West B, Brown RM, Kirchhoff J, Raymond CR, et al. The mGlu5 receptor regulates extinction of cocaine-driven behaviours. Drug and Alcohol Dependence. 2014; 137 (0) 83–9. [PubMed: 24576814]
9. Miller CA, Marshall JF. Molecular Substrates for Retrieval and Reconsolidation of Cocaine-Associated Contextual Memory. Neuron. 2005; 47 (6) 873–84. [PubMed: 16157281]
10. Jones B, Bukoski E, Nadel L, Fellous J-M. Remaking memories: Reconsolidation updates positively motivated spatial memory in rats. Learning & Memory. 2012; 19 (3) 91–8. [PubMed: 22345494]
11. Monfils M-H, Cowansage KK, Klann E, LeDoux JE. Extinction-Reconsolidation Boundaries: Key to Persistent Attenuation of Fear Memories. Science. 2009; 324 (5929) 951–5. [PubMed: 19342552]
12. Otis JM, Werner CT, Mueller D. Noradrenergic Regulation of Fear and Drug-Associated Memory Reconsolidation. Neuropsychopharmacology. 2014.
13. Lee TH, Szabo ST, Fowler JC, Mannelli P, Mangum OB, Beyer WF, et al. Pharmacologically-mediated reactivation and reconsolidation blockade of the psychostimulant-abuse circuit: a novel treatment strategy. Drug Alcohol Depend. 2012; 124 (1–2) 11–8. [PubMed: 22356892]
14. Lee JL, Di Ciano P, Thomas KL, Everitt BJ. Disrupting reconsolidation of drug memories reduces cocaine-seeking behavior. Neuron. 2005; 47 (6) 795–801. [PubMed: 16157275]
15. Childress AR, Hole AV, Ehrman RN, Robbins SJ, McLellan AT, O'Brien CP. Cue reactivity and cue reactivity interventions in drug dependence. NIDA Res Monogr. 1993; 137: 73–95. [PubMed: 8289929]
16. Young EJ, Aceti M, Griggs EM, Fuchs RA, Zigmond Z, Rumbaugh G, et al. Selective, retrieval-independent disruption of methamphetamine-associated memory by actin depolymerization. Biological psychiatry. 2014; 75 (2) 96–104. [PubMed: 24012327]
17. Kasai H, Fukuda M, Watanabe S, Hayashi-Takagi A, Noguchi J. Structural dynamics of dendritic spines in memory and cognition. Trends in Neurosciences. 2010; 33 (3) 121–9. [PubMed: 20138375]
18. Lai CSW, Franke TF, Gan W-B. Opposite effects of fear conditioning and extinction on dendritic spine remodelling. Nature. 2012; 483 (7387) 87–91. [PubMed: 22343895]
19. Yang G, Pan F, Gan W-B. Stably maintained dendritic spines are associated with lifelong memories. Nature. 2009; 462 (7275) 920–4. [PubMed: 19946265]
20. Kasai H, Matsuzaki M, Noguchi J, Yasumatsu N, Nakahara H. Structure–stability–function relationships of dendritic spines. Trends in Neurosciences. 2003; 26 (7) 360–8. [PubMed: 12850432]
21. Smart FM, Halpain S. Regulation of dendritic spine stability. Hippocampus. 2000; 10 (5) 542–54. [PubMed: 11075824]
22. Star EN, Kwiatkowski DJ, Murthy VN. Rapid turnover of actin in dendritic spines and its regulation by activity. Nat Neurosci. 2002; 5 (3) 239–46. [PubMed: 11850630]
23. Kim C-H, Lisman JE. A Role of Actin Filament in Synaptic Transmission and Long-Term Potentiation. The Journal of Neuroscience. 1999; 19 (11) 4314–24. [PubMed: 10341235]
24. Lin B, Kramár EA, Bi X, Brucher FA, Gall CM, Lynch G. Theta Stimulation Polymerizes Actin in Dendritic Spines of Hippocampus. The Journal of Neuroscience. 2005; 25 (8) 2062–9. [PubMed: 15728846]
25. Rex CS, Gavin CF, Rubio MD, Kramar EA, Chen LY, Jia Y, et al. Myosin IIb Regulates Actin Dynamics during Synaptic Plasticity and Memory Formation. Neuron. 2010; 67 (4) 603–17. [PubMed: 20797537]
26. Krucker T, Siggins GR, Halpain S. Dynamic actin filaments are required for stable long-term potentiation (LTP) in area CA1 of the hippocampus. Proceedings of the National Academy of Sciences. 2000; 97 (12) 6856–61.
27. Mantzur L, Joels G, Lamprecht R. Actin polymerization in lateral amygdala is essential for fear memory formation. Neurobiology of Learning and Memory. 2009; 91 (1) 85–8. [PubMed: 18812227]

28. Rehberg K, Bergado-Acosta JR, Koch JC, Stork O. Disruption of fear memory consolidation and reconsolidation by actin filament arrest in the basolateral amygdala. Neurobiology of Learning and Memory. 2010; 94 (2) 117–26. [PubMed: 20416387]
29. Fischer A, Sananbenesi F, Schrick C, Spiess J, Radulovic J. Distinct Roles of Hippocampal De Novo Protein Synthesis and Actin Rearrangement in Extinction of Contextual Fear. The Journal of Neuroscience. 2004; 24 (8) 1962–6. [PubMed: 14985438]
30. Gavin CF, Rubio MD, Young E, Miller C, Rumbaugh G. Myosin II motor activity in the lateral amygdala is required for fear memory consolidation. Learning & Memory. 2012; 19 (1) 9–14. [PubMed: 22174310]
31. Rosenfeld SS, Xing J, Chen LQ, Sweeney HL. Myosin IIb is unconventionally conventional. J Biol Chem. 2003; 278 (30) 27449–55. [PubMed: 12740390]
32. Miller CA, Marshall JF. Altered prelimbic cortex output during cue-elicited drug seeking. The Journal of neuroscience: the official journal of the Society for Neuroscience. 2004; 24 (31) 6889–97. [PubMed: 15295023]
33. Aguilar-Valles A, Vaissiere T, Griggs EM, Mikaelsson MA, Takacs IF, Young EJ, et al. Methamphetamine-Associated Memory Is Regulated by a Writer and an Eraser of Permissive Histone Methylation. Biological psychiatry. 2013.
34. Langmead B, Trapnell C, Pop M, Salzberg SL. Ultrafast and memory-efficient alignment of short DNA sequences to the human genome. Genome biology. 2009; 10 (3) R25. [PubMed: 19261174]
35. Trapnell C, Pachter L, Salzberg SL. TopHat: discovering splice junctions with RNA-Seq. Bioinformatics. 2009; 25 (9) 1105–11. [PubMed: 19289445]
36. Anders S, Huber W. Differential expression analysis for sequence count data. Genome biology. 2010; 11 (10) R106. [PubMed: 20979621]
37. Griggs EM, Young EJ, Rumbaugh G, Miller CA. MicroRNA-182 regulates amygdala-dependent memory formation. The Journal of neuroscience: the official journal of the Society for Neuroscience. 2013; 33 (4) 1734–40. [PubMed: 23345246]
38. Guissouma H, Froidevaux MS, Hassani Z, Demeneix BA. In vivo siRNA delivery to the mouse hypothalamus confirms distinct roles of TR beta isoforms in regulating TRH transcription. Neuroscience letters. 2006; 406 (3) 240–3. [PubMed: 16930836]
39. McQuown SC, Barrett RM, Matheos DP, Post RJ, Rogge GA, Alenghat T, et al. HDAC3 is a critical negative regulator of long-term memory formation. The Journal of neuroscience: the official journal of the Society for Neuroscience. 2011; 31 (2) 764–74. [PubMed: 21228185]
40. Miller CA, Marshall JF. Altered Fos expression in neural pathways underlying cue-elicited drug seeking in the rat. The European journal of neuroscience. 2005; 21 (5) 1385–93. [PubMed: 15813948]
41. Stinus L, Cador M, Zorrilla EP, Koob GF. Buprenorphine and a CRF1 antagonist block the acquisition of opiate withdrawal-induced conditioned place aversion in rats. Neuropsychopharmacology: official publication of the American College of Neuropsychopharmacology. 2005; 30 (1) 90–8. [PubMed: 15138444]
42. Mead AN, Stephens DN. CNQX but not NBQX prevents expression of amphetamine-induced place preference conditioning: a role for the glycine site of the NMDA receptor, but not AMPA receptors. The Journal of pharmacology and experimental therapeutics. 1999; 290 (1) 9–15. [PubMed: 10381753]
43. Newton PM, Orr CJ, Wallace MJ, Kim C, Shin HS, Messing RO. Deletion of N-type calcium channels alters ethanol reward and reduces ethanol consumption in mice. The Journal of neuroscience: the official journal of the Society for Neuroscience. 2004; 24 (44) 9862–9. [PubMed: 15525770]
44. Munoz-Cuevas FJ, Athilingam J, Piscopo D, Wilbrecht L. Cocaine-induced structural plasticity in frontal cortex correlates with conditioned place preference. Nature neuroscience. 2013; 16 (10) 1367–9. [PubMed: 23974707]
45. Kovács M, Tóth J, Hetényi C, Málnási-Csizmadia A, Sellers JR. Mechanism of Blebbistatin Inhibition of Myosin II. Journal of Biological Chemistry. 2004; 279 (34) 35557–63. [PubMed: 15205456]

46. Fuchs RA, Evans KA, Ledford CC, Parker MP, Case JM, Mehta RH, et al. The Role of the Dorsomedial Prefrontal Cortex, Basolateral Amygdala, and Dorsal Hippocampus in Contextual Reinstatement of Cocaine Seeking in Rats. Neuropsychopharmacology. 2004; 30 (2) 296–309.
47. Wells AM, Arguello AA, Xie X, Blanton MA, Lasseter HC, Reittinger AM, et al. Extracellular Signal-Regulated Kinase in the Basolateral Amygdala, but not the Nucleus Accumbens Core, is Critical for Context-Response-Cocaine Memory Reconsolidation in Rats. Neuropsychopharmacology. 2013; 38 (5) 753–62. [PubMed: 23232446]
48. Reichel CM, See RE. Modafinil effects on reinstatement of methamphetamine seeking in a rat model of relapse. Psychopharmacology. 2010; 210 (3) 337–46. [PubMed: 20352413]
49. Rubio FJ, Liu QR, Li X, Cruz FC, Leao RM, Warren BL, et al. Context-induced reinstatement of methamphetamine seeking is associated with unique molecular alterations in fos-expressing dorsolateral striatum neurons. The Journal of neuroscience: the official journal of the Society for Neuroscience. 2015; 35 (14) 5625–39. [PubMed: 25855177]
50. Bond LM, Tumbarello DA, Kendrick-Jones J, Buss F. Small-molecule inhibitors of myosin proteins. Future Med Chem. 2013; 5 (1) 41–52. [PubMed: 23256812]
51. Wang X, Chong M, Wang H, Zhang J, Xu H, Liu D. Block the function of nonmuscle myosin II by blebbistatin induces zebrafish embryo cardia bifida. In Vitro Cell Dev Biol Anim. 2014.
52. Eddinger TJ, Meer DP, Miner AS, Meehl J, Rovner AS, Ratz PH. Potent inhibition of arterial smooth muscle tonic contractions by the selective myosin II inhibitor, blebbistatin. The Journal of pharmacology and experimental therapeutics. 2007; 320 (2) 865–70. [PubMed: 17132816]
53. Rubio MD, Johnson R, Miller CA, Huganir RL, Rumbaugh G. Regulation of synapse structure and function by distinct myosin II motors. The Journal of neuroscience: the official journal of the Society for Neuroscience. 2011; 31 (4) 1448–60. [PubMed: 21273429]
54. Cheng D, Hoogenraad CC, Rush J, Ramm E, Schlager MA, Duong DM, et al. Relative and absolute quantification of postsynaptic density proteome isolated from rat forebrain and cerebellum. Mol Cell Proteomics. 2006; 5 (6) 1158–70. [PubMed: 16507876]
55. Peng J, Kim MJ, Cheng D, Duong DM, Gygi SP, Sheng M. Semiquantitative proteomic analysis of rat forebrain postsynaptic density fractions by mass spectrometry. J Biol Chem. 2004; 279 (20) 21003–11. [PubMed: 15020595]
56. Ertl P, Rohde B, Selzer P. Fast Calculation of Molecular Polar Surface Area as a Sum of Fragment-Based Contributions and Its Application to the Prediction of Drug Transport Properties. Journal of Medicinal Chemistry. 2000; 43 (20) 3714–7. [PubMed: 11020286]
57. Hitchcock SA, Pennington LD. Structure–Brain Exposure Relationships. Journal of Medicinal Chemistry. 2006; 49 (26) 7559–83. [PubMed: 17181137]
58. Crawley, JN. What's Wrong With My Mouse: Behavioral Phenotyping of Transgenic and Knockout Mice. 2nd. Wiley Press; 2007. 44–57.
59. Feng G, Mellor RH, Bernstein M, Keller-Peck C, Nguyen QT, Wallace M, et al. Imaging Neuronal Subsets in Transgenic Mice Expressing Multiple Spectral Variants of GFP. Neuron. 2000; 28 (1) 41–51. [PubMed: 11086982]
60. Heinrichs SC, Leite-Morris KA, Guy MD, Goldberg LR, Young AJ, Kaplan GB. Dendritic structural plasticity in the basolateral amygdala after fear conditioning and its extinction in mice. Behavioural brain research. 2013; 248: 80–4. [PubMed: 23570859]
61. Pignataro A, Middei S, Borreca A, Ammassari-Teule M. Indistinguishable pattern of amygdala and hippocampus rewiring following tone or contextual fear conditioning in C57BL/6 mice. Frontiers in behavioral neuroscience. 2013; 7: 156. [PubMed: 24194705]
62. Medeiros NA, Burnette DT, Forscher P. Myosin II functions in actin-bundle turnover in neuronal growth cones. Nat Cell Biol. 2006; 8 (3) 216–26.
63. Daley, DC, Mercer, D. Therapy Manuals for Drug Addiction. Bethesda: NIH; 2002.
64. Tran-Nguyen LT, Fuchs RA, Coffey GP, Baker DA, O'Dell LE, Neisewander JL. Time-dependent changes in cocaine-seeking behavior and extracellular dopamine levels in the amygdala during cocaine withdrawal. Neuropsychopharmacology: official publication of the American College of Neuropsychopharmacology. 1998; 19 (1) 48–59. [PubMed: 9608576]

65. West EA, Saddoris MP, Kerfoot EC, Carelli RM. Prelimbic and infralimbic cortical regions differentially encode cocaine-associated stimuli and cocaine-seeking before and following abstinence. Eur J Neurosci. 2014; 39 (11) 1891–902. [PubMed: 24690012]

66. Grimm JW, Hope BT, Wise RA, Shaham Y. Neuroadaptation. Incubation of cocaine craving after withdrawal. Nature. 2001; 412 (6843) 141–2. [PubMed: 11449260]

67. Grimm JW, Lu L, Hayashi T, Hope BT, Su TP, Shaham Y. Time-dependent increases in brain-derived neurotrophic factor protein levels within the mesolimbic dopamine system after withdrawal from cocaine: implications for incubation of cocaine craving. The Journal of neuroscience: the official journal of the Society for Neuroscience. 2003; 23 (3) 742–7. [PubMed: 12574402]

68. Lee BR, Ma YY, Huang YH, Wang X, Otaka M, Ishikawa M, et al. Maturation of silent synapses in amygdala-accumbens projection contributes to incubation of cocaine craving. Nat Neurosci. 2013; 16 (11) 1644–51. [PubMed: 24077564]

69. Ma YY, Lee BR, Wang X, Guo C, Liu L, Cui R, et al. Bidirectional modulation of incubation of cocaine craving by silent synapse-based remodeling of prefrontal cortex to accumbens projections. Neuron. 2014; 83 (6) 1453–67. [PubMed: 25199705]

70. Straight AF, Cheung A, Limouze J, Chen I, Westwood NJ, Sellers JR, et al. Dissecting temporal and spatial control of cytokinesis with a myosin II Inhibitor. Science. 2003; 299 (5613) 1743–7. [PubMed: 12637748]

71. Kepiro M, Varkuti BH, Vegner L, Voros G, Hegyi G, Varga M, et al. para-Nitroblebbistatin, the non-cytotoxic and photostable myosin II inhibitor. Angew Chem Int Ed Engl. 2014; 53 (31) 8211–5. [PubMed: 24954740]

72. Hawrylycz MJ, Lein ES, Guillozet-Bongaarts AL, Shen EH, Ng L, Miller JA, et al. An anatomically comprehensive atlas of the adult human brain transcriptome. Nature. 2012; 489 (7416) 391–9. [PubMed: 22996553]

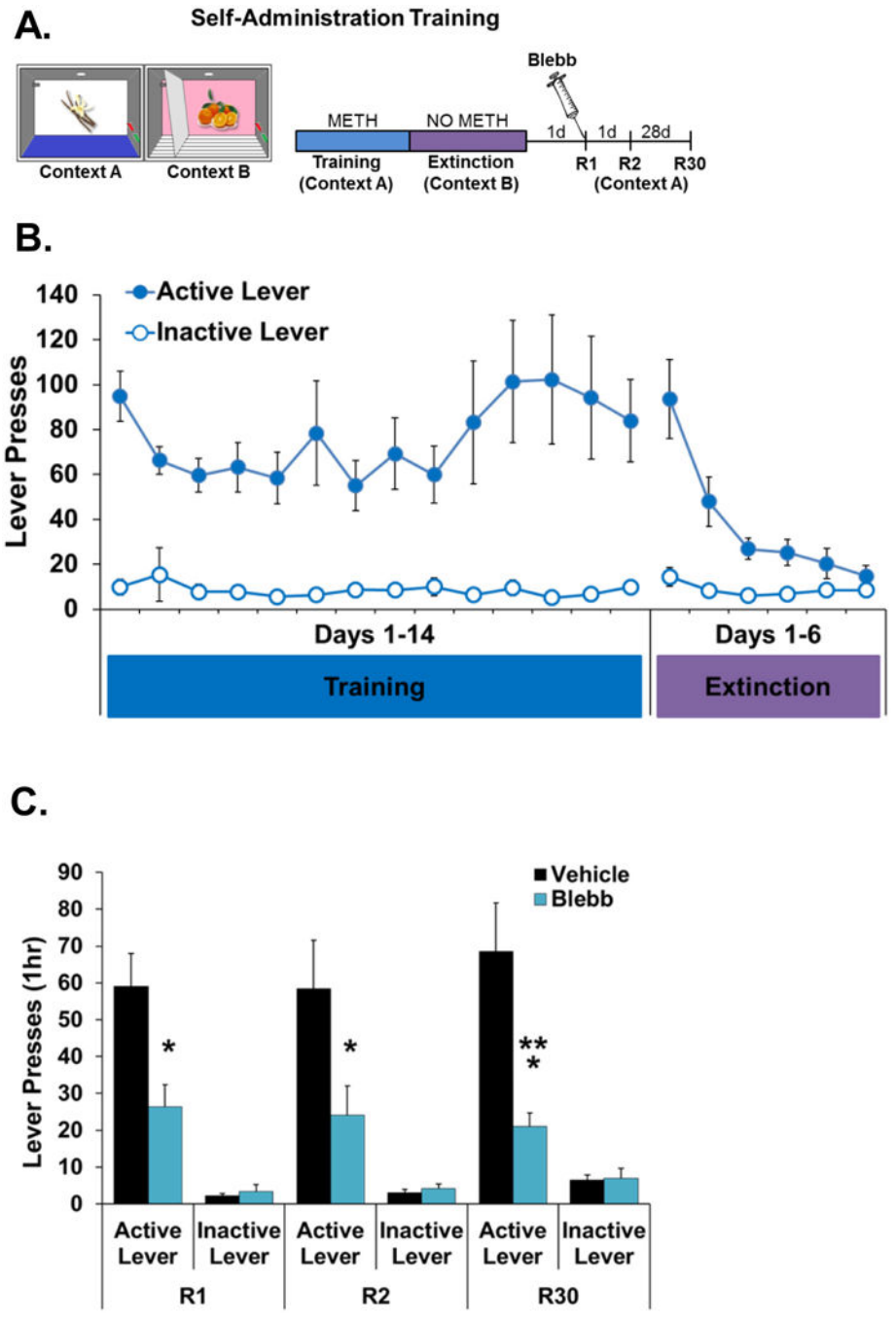

Figure 1.

(A) Schematic of experiment design for context-induced reinstatement of instrumental METH seeking. **(B)** Animals learned the association between the active lever and METH reinforcement in Context A and subsequently underwent extinction of active lever pressing in Context B. **(C)** The immediate disruption of context-induced METH seeking by a single intra-BLC Blebb treatment prior to reinstatement test 1 (R1) persisted for at least 30 days (R30). Vehicle was the inactive enantiomer of Blebb. Error bars represent SEM and * $P \leq 0.05$, *** $P \leq 0.0005$ for Veh (N=5) vs Blebb (N=9) active lever presses.

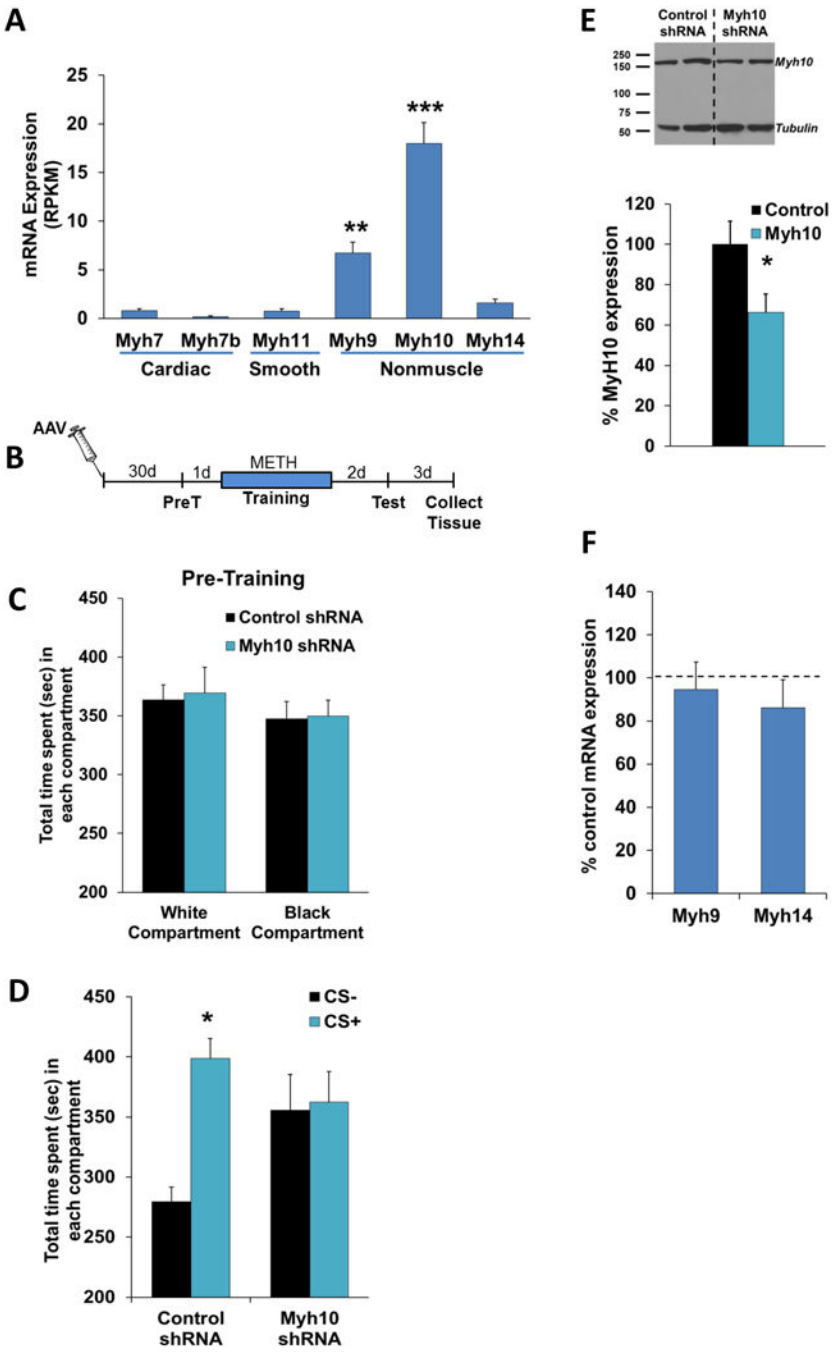

Figure 2.

Relative expression of nonmuscle myosin IIB in the BLC and its contribution to METH-associated memory. **(A)** RPKM values from RNA-Seq on BLC tissue for the Class II myosins targeted by Blebb and expressed in the BLC (N=4). Posthoc comparisons indicate that *Myh10* is greater than all other *Myh*'s, ***p≤0.0001 and *Myh9* is greater than all other *Myh*'s, except *Myh10*, **p≤0.05. **(B)** Schematic of experiment design for shRNA knockdown of *Myh10* prior to METH CPP. **(C)** Knocking down *Myh10* had no effect on pre-training compartment preference. **(D)** Knocking down *Myh10* disrupted METH-

associated memory (Control, N=16; *Myh10* siRNA N=10), * $P \leq 0.05$ for CS+ vs CS−. **(E)** MYH10 was significantly reduced in the BLC of animals that received the *Myh10* shRNA-AAV, * $P \leq 0.05$ for Control vs Myh10 shRNA. **(F)** Knocking down *Myh10* had no effect on BLC levels of the NMIIA or IIC heavy chains, *Myh9* and *Myh14* (Control, N=5; *Myh10* shRNA, N=5). Error bars represent SEM.

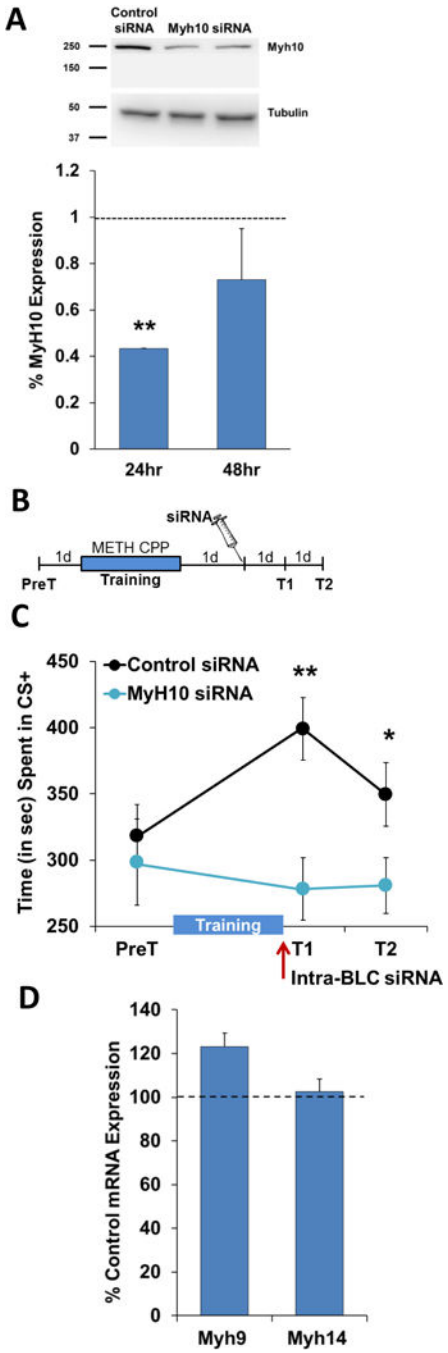

Figure 3.

Post-consolidation loss of nonmuscle myosin IIB produces a lasting disruption of METH-associated memory. **(A)** siRNA-mediated knockdown of *Myh10* decreased the MYH10 protein expression within 24 hours, ** $P \leq 0.005$ for Control vs *Myh* siRNA. **(B)** Schematic of experimental design. **(C)** siRNA-mediated, post-memory consolidation knockdown of *Myh10* disrupted METH-associated memory, * $P \leq 0.05$, ** $P \leq 0.005$ for Control (N=9) vs *Myh10* (N=11) siRNA. **(D)** Knocking down *Myh10* had no effect on BLC levels of the NMIIA or IIC heavy chains, *Myh9* and *Myh14*. Error bars represent SEM.

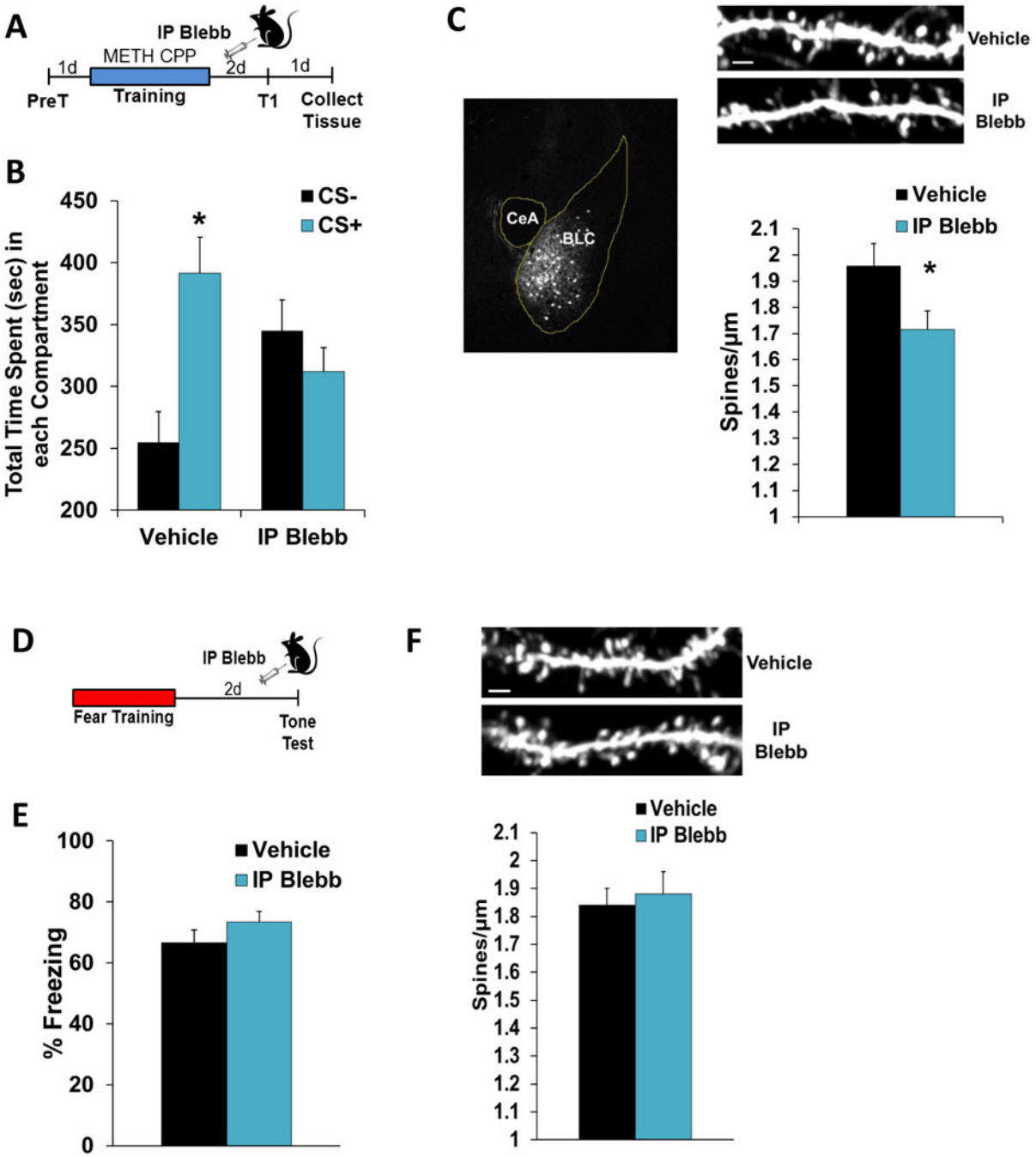

Figure 4.

Selective targeting of METH, but not fear-associated memory and BLC spines by systemic myosin II inhibition. **(A)** Schematic of experiment design for systemic Blebb delivery (IP) prior to testing for METH-associated memory. **(B)** Consolidated METH-associated memories were disrupted by systemic myosin II inhibition (Veh, N=15; Blebb, N=14), * $P \leq 0.05$ for CS+ vs CS−. Vehicle was the inactive enantiomer of Blebb. **(C)** Representative images of Thy1-GFP(m) expression in the BLC and spine density from animals with behavior depicted in (B); * $P \leq 0.05$ for Veh (N=6) vs IP Blebb (N=6). Scale bar is equal

to 2μm. **(D)** Schematic of experiment design for systemic Blebb delivery (IP) prior to testing for auditory fear memory. Systemic inhibition of myosin II had no effect on **(E)** consolidated fear memory (Veh, N=13; IP Blebb, N=13) or **(F)** BLC spine density (Veh, N=5; IP Blebb, N=5) when delivered prior to testing. Error bars represent SEM.

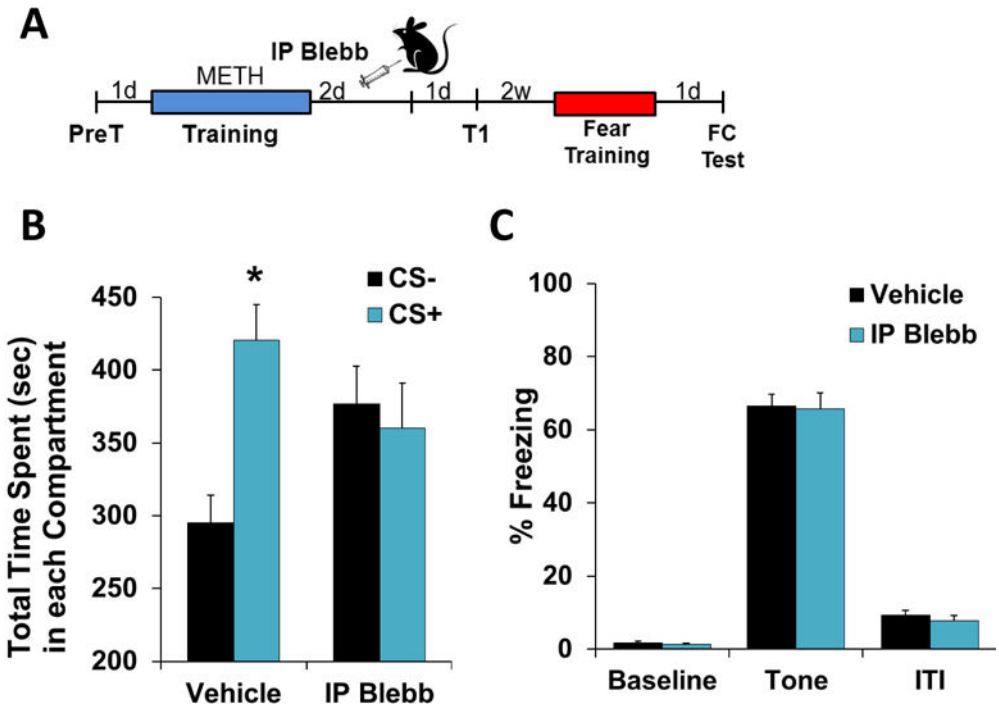

Figure 5.

Systemic Blebb delivery disrupts METH-associated memory storage without retrieval. **(A)** Schematic of experimental design. **(B)** METH-associated memory was absent twenty-four hours after home cage delivery of Blebb (IP) (Veh, N=7); Blebb, N=8), * $P \lesssim 0.05$ for CS+ vs CS−. Vehicle was the inactive enantiomer of Blebb. **(C)** Prior memory disruption by systemic Blebb treatment did not affect future learning. Error bars represent SEM.